Proceedings of the
International Conference on Mechanical Engineering 2007
(ICME2007) 29- 31 December 2007, Dhaka, Bangladesh

ICME07-TH-36

An Analytical Study of Heat Transfer during Jet Impingement Quenching

M A Islam[1], M Monde[2]and P Roy[1]

[1]Department of Mechanical Engineering, BUET, Dhaka-1000, BANGLADESH
aislam@me.buet.ac.bd
[2]Department of Mechanical Engineering, Saga University,
1 Honjo-machi, Saga 849-8502, JAPAN

ABSTRACT

The phenomenon that happens during a brief contact of a water jet impinging on a hot surface has been analytically investigated. A simple semi-infinite conduction heat transfer model is considered in this case and the heat transfer analysis has been carried out for three heating processes of the impinging liquid, namely with (i) prescribed surface temperature (PST-case), (ii) prescribed surface heat flux (PHF-case) and (iii) time-dependent surface temperature (TST-case). For each of three processes, average liquid temperature and average internal energy equations have been derived as a function of liquid depth equal to the critical diameter of vapor embryo and time. These equations are solved numerically and their upshots are discussed.

Keywords: Heat Conduction, Jet Impingement Quenching, Semi-infinite solid.

1. INTRODUCTION

Jet impingement quenching has the larger cooling potential and is a very effective means of cooling for many applications. It is very important in LOCA (Loss of coolant accident) analysis, steel manufacturing, metallurgy, microelectronic device making and thermal management processes. It may be useful in elucidating poorly understood phenomena such as Leidenfrost phenomenon and homogeneous nucleation. A comprehensive review of jet impingement boiling was made by Wolf et al. [1]. They observed that in contrast to research on nucleate boiling and critical heat flux, there is a scarcity of concrete studies relating to jet impingement for the film boiling and transition regimes.

Jet impingement cooling of a hot surface may give rise to heterogeneous and/or homogeneous nucleation of bubbles, which is yet to be explored. A number of interesting phenomena have been reported for jet impingement quenching. Piggot et al. [2] reported a delay to the movement of the wetting front during quenching heated rods from an initial temperature of 700^{o}C with a sub-cooled water jet. The quench began with quiet film boiling and then a white patch around 5 mm in diameter appeared beneath the jet. The liquid film then broke into tiny droplets in a spray pattern, which was followed by an oscillating liquid sheet that lifted from the surface of the rod. Finally the wetting front moved forward over the heated surface. Some recent works include Hammad et al. [3], Woodfield et al. [4], Mozumder et al. [5] and Islam et al. [6-7]. Most of these recent studies have been performed by quenching a cylindrical block of initial temperatures ranging from 250-400^{o}C. These studies included flow visualization, surface temperature, surface heat flux, cooling curves, boiling curves, resident time (wetting delay) and boiling sound. Most recently Islam et al. [8] reported some excellent video images at early stages of jet impingement quenching and demonstrated a clue towards development of a model of heat transfer. Therefore, the nature of the phase change phenomena and characteristics of heat transfer for impinging jets at early stages in the high temperature context is yet to be understood clearly.

A theoretical model to elucidate the heat conduction phenomena during jet impingement quenching has been developed in this study. The equations are solved analytically and the results are articulated to get a better view of the observable fact.

2. ANALYSIS METHODOLOGY

2.1 Model

Liquid in brief contact with the hot solid during jet impingement quenching can be considered as one dimensional semi-infinite solid through which heat from the hot solid is conducted. Therefore, a simple conduction analysis can find the temperature distribution within the liquid. The temperature distribution is dependent on the jet temperature, the interface temperature, the thermal diffusivity of both liquid and solid, the depth of liquid from the solid surface and the time of brief contact.

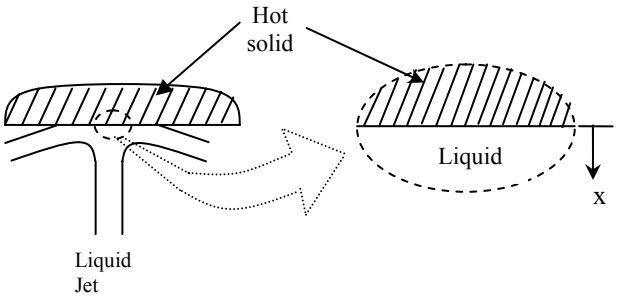

Fig 1: Schematic of jet impingement quenching and semi-infinite liquid

The governing equation of the model is given by

$$\frac{\partial^2 T}{\partial x^2} = \frac{1}{a}\frac{\partial T}{\partial t} \quad \text{for } 0 < x < \infty \tag{1}$$

The boundary condition at x=0 can be either of the following types:

(i) Prescribe surface temperature (PST)

$T = T_i$

(ii) Prescribed surface heat flux (PHF)

$$-\lambda\frac{\partial T}{\partial x} = q_0$$

(iii) Time dependent surface temperature (TST)

$T = kt$

The initial condition is

$T=T_l$ for $0 < x < \infty$.

where T_l is the jet temperature, T_i is the interface temperature, a is the thermal diffusivity of liquid, λ is the thermal conductivity of solid, q_0 is the surface heat flux, k is a constant representing the rate of change in surface temperature, x is the depth of liquid from the solid surface and t is the time elapsed after jet comes in contact with the surface. The interface temperature, T_i mentioned above is calculated according to Carslaw and Jaeger [9] using Eq. (2).

$$\frac{T_s - T_i}{T_i - T_l} = \sqrt{\frac{(\rho c\lambda)_l}{(\rho c\lambda)_s}} \tag{2}$$

where, T_s is the surface temperature of solid, 'ρ', 'c' and 'λ' are, respectively, the density, specific heat, and thermal conductivity and the subscripts 'l' and 's' stand for liquid and solid respectively. Depending on boundary conditions three different cases are described below:

2.1.1 Prescribed Surface Temperature (PST) Case

The temperature distribution within the liquid is given by the following equation:

$$T(x,t) = T_l + (T_i - T_l)\,\mathrm{erfc}\,(x/\sqrt{4at}) \tag{3}$$

The amount of energy stored in the superheated liquid with reference to saturated liquid is

$$u(x,t) = c\left(T(x,t) - T_0\right) \tag{4}$$

where, c is the specific heat of the liquid and T_0 is the reference temperature, which can reasonably be the saturation temperature at ambient pressure.

The average of the stored energy over the depth of the liquid is

$$\bar{u}(x_e,t) = \frac{1}{x_e}\int_0^{x_e} u(x,t)dx \tag{5}$$

where, x_e is the liquid depth equal to the diameter of the critical vapor embryo in the superheated liquid. The value of x_e ($=2r_e$) is not known. It depends on the liquid temperature which in turn depends on the contact time t. The equilibrium embryo size is given by Eq. (6) according to Carey [10].

$$r_e = \frac{2\sigma}{P_{sat}(\bar{T})\exp[v_l\{P_\infty - P_{sat}(\bar{T})\}/R\bar{T}] - P_\infty} \tag{6}$$

Eq. (5) can be simplified as follows.

$$\bar{u}(x_e,t) = c(T_l - T_0) + \frac{c(T_i - T_l)}{(x_e/\sqrt{4at})}\left(\frac{1}{\sqrt{\pi}} - \mathrm{ierfc}(x_e/\sqrt{4at})\right) \tag{7}$$

Here,

$$\mathrm{ierfc}(x_e/\sqrt{4at}) = \frac{1}{\sqrt{\pi}}\exp(-x_e^2/4at) - \frac{x_e}{\sqrt{4at}}\mathrm{erfc}(x_e/\sqrt{4at})$$

In order to get an estimate of x_e, the average temperature of the liquid over a certain volume of the liquid in contact is considered as given in the following equation:

$$\bar{T}(x_e,t) = \frac{1}{x_e}\int_0^{x_e} T(x,t)dx \tag{8}$$

Eq. (8) can be manipulated analytically to have a simplified shape as follows:

$$\bar{T}(x_e,t) = T_l + (T_i - T_l)\frac{\sqrt{4at}}{x_e}\left(\frac{1}{\sqrt{\pi}} - \mathrm{ierfc}(x_e/\sqrt{4at})\right) \tag{9}$$

Eq. (7) can be simplified using average liquid temperature as follows:

$$\bar{u}(x_e,t) = c\left(\bar{T}(x_e,t) - T_0\right) \tag{10}$$

2.1.2 Prescribed Surface Heat Flux (PHF) Case

The temperature distribution within the liquid is given by the following equation:

$$T(x,t) = T_l + \frac{q_0\sqrt{4at}}{\lambda}\mathrm{ierfc}(x/\sqrt{4at}) \tag{11}$$

where,

$$\mathrm{ierfc}(x/\sqrt{4at}) = \frac{1}{\sqrt{\pi}}\exp(-x^2/4at) - \frac{x}{\sqrt{4at}}\mathrm{erfc}(x/\sqrt{4at})$$

and q_o is the uniform surface heat flux. The average temperature distribution has the following simplified form:

$$\bar{T}(x_e,t) = T_l + \frac{q_0\sqrt{4at}}{(x_e/\sqrt{4at})\lambda}\left(\frac{1}{4} - i^2\mathrm{erfc}(x_e/\sqrt{4at})\right) \tag{12}$$

where,

$$i^2\mathrm{erfc}(x_e/\sqrt{4at}) = \frac{1}{4}\left[\mathrm{erfc}(x_e/\sqrt{4at}) - 2x_e\,\mathrm{ierfc}(x_e/\sqrt{4at})\right]$$

The average of the stored energy can be calculated by Eq. (10) as before.

2.1.3 Time dependent surface temperature (TST) case

The temperature distribution within the liquid is given by the following equation:

$$T(x,t) = T_l + 4kti^2erfc(x/\sqrt{4at}) \qquad (13)$$

where,

$$i^2erfc(x/\sqrt{4at}) = \frac{1}{4}\left[erfc(x/\sqrt{4at}) - 2xierfc(x/\sqrt{4at})\right]$$

The average temperature distribution has the following simplified form:

$$\bar{T}(x_e,t) = T_l + \frac{kt}{(x_e/\sqrt{4at})}\left(\frac{2}{3\sqrt{\pi}} - 4i^3erfc(x_e/\sqrt{4at})\right) \qquad (14)$$

where,

$$i^3erfc(x_e/\sqrt{4at}) = \frac{1}{6}\left[ierfc(x_e/\sqrt{4at}) - 2x_e i^2erfc(x_e/\sqrt{4at})\right]$$

The average of the stored energy can be calculated by Eq. (10) as before.

2.2 Solution Procedure

The values of q_0 and k are taken as 134 MW/m^2 and 37.7 x 10^6 K/s, respectively, from Iida et al. [11].

Following steps are followed to calculate $\bar{T}$ and $\bar{u}$:

(i) For any time t, an initial guess is made for x_e.
(ii) Properties are taken at 100°C and x_e is stored as x_{eold}.
(iii) Using Eq (8), $\bar{T}$ is calculated and properties are again taken at $\bar{T}$.
(iv) Using Eq. (6), the value of r_e is computed and then x_e is taken to be $2r_e$.
(v) Step (ii) is repeated until absolute value of $(x_e - x_{eold})/x_{eold}$ is less than 0.0001.
(vi) $\bar{u}$ is calculated using Eq. (10)
(vii) The values of t, re, xe, $\bar{T}$ and $\bar{u}$ are recorded.
(viii) The value of time is incremented and then steps (ii) to (vii) are repeated.

The flow chart of the algorithm has been given in the appendix.

3. RESULTS AND DISCUSSIONS

The temperature of the liquid impinging on the hot surface has been taken as 50°C in making comparison among different cases.

Fig.2 shows the variation of average liquid temperature, $\bar{T}$ (which is shown as T_{lavg}) with time t for three different cases as explained in section 2.1. For PST case, $\bar{T}$ is above 300°C for the contact times in the range from 0.1 μs to 10 μs as shown in Fig. 2. For PHF case and TST case, the value of $\bar{T}$ exceeds 300°C for contact times 8 μs and 10 μs, respectively. The rate of change in $\bar{T}$ is greater for TST case than for PHF case. For example, after 10 μs the value of $\bar{T}$ is about 420°C in TST case and 300°C in PHF case.

Fig.3 shows the variation of equilibrium radius of vapor embryo, r_e with time, t for different cases. For PST case, steady and converged solution for r_e is achieved within 0.1 μs. For PHF case and TST case, although solutions are found after 2 μs and 3.5 μs respectively, steady values of r_e are attained after 10 μs.

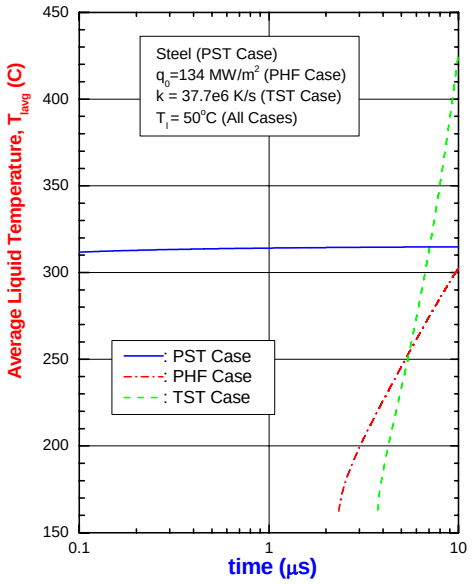

Fig 2: Variation of Average Liquid Temperature

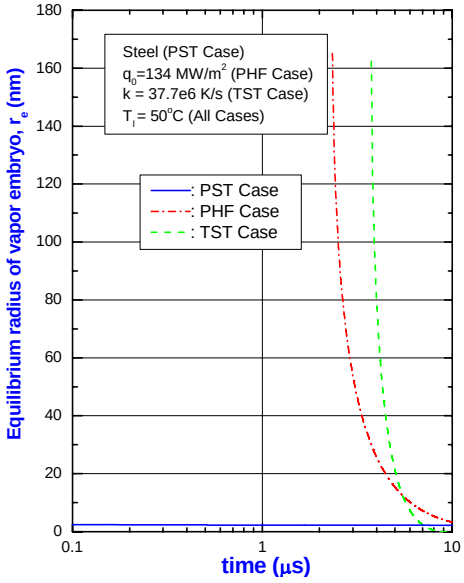

Fig 3: Variation of Equilibrium radius of vapor embryo

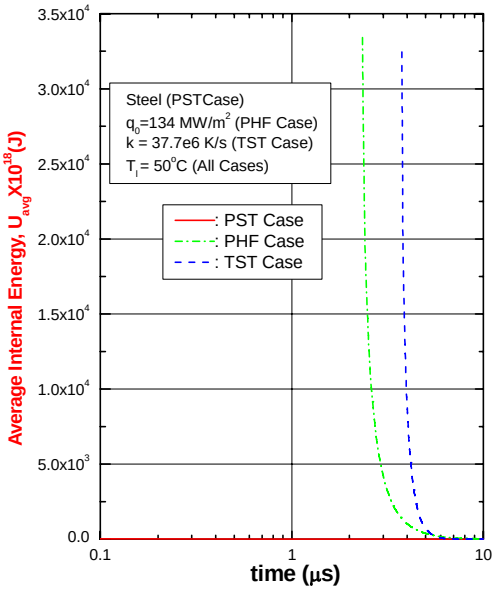

Fig 4: Variation of average internal energy.

Fig. 4 shows the variation of average internal energy, U_{avg} with time, t for different cases. For PST case, U_{avg} is invariable in the time range (0.1 μs to 10 μs). For PHF and TST case, U_{avg} reaches a stable value after 10 μs. The value of U_{avg} necessary for homogeneous bubble formation is not known yet and it certainly needs careful study [8].

Fig. 5 shows the variation of liquid temperature with liquid depth, x for different cases at 0.5 μs. Even though liquid temperature decreases linearly with liquid depth for all cases, their values and decreasing rates are different.

Fig.6 shows the effect of liquid initial temperature, T_l on variation of average liquid temperature, T_{lavg} with time, t for TST case. As T_l increases, T_{lavg} vs t curve shifts to the left which indicates that for a fixed value of t, T_{lavg} increases with T_l. Change of T_l has the same effect on other cases.

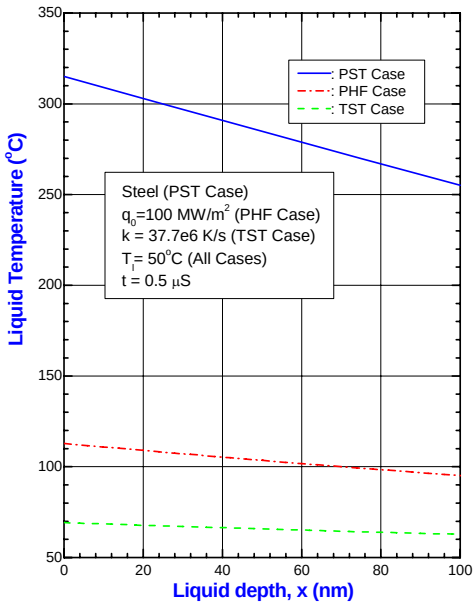

Fig 5: Variation of liquid temperature with liquid depth

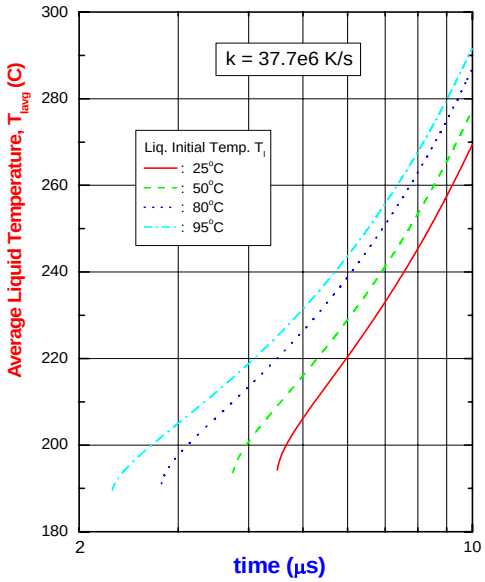

Fig 6: Effect of initial jet temperature on average liquid temperature for TST case.

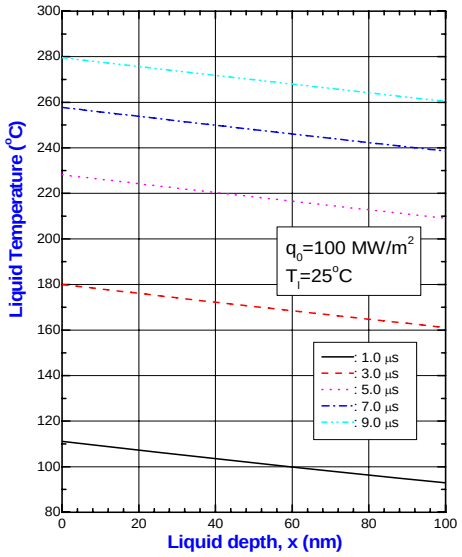

Fig 7: Effect of contact time on the temperature distribution (PHF Case)

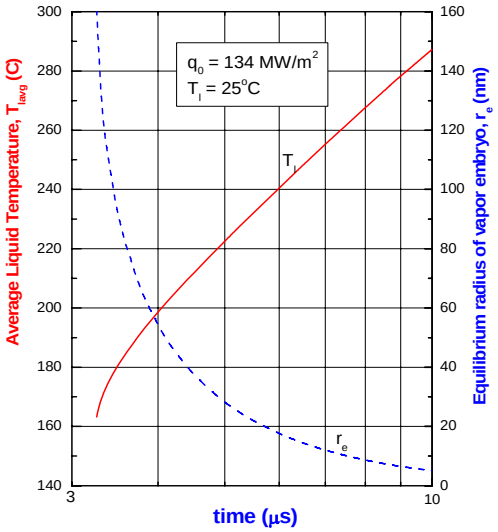

Fig 8: Variation of average liquid temperature and equilibrium radius of vapor embryo for PHF case

Fig.7 shows the effect of time, t on variation of liquid temperature with liquid depth, x for PHF case. The liquid initial temperature is 25°C. For a preset value of x, the liquid instantaneous temperature increases with time. Similar effect of time has been observed for other cases.

Fig. 8 shows the variation of T_{lavg} and r_e with time for PHF case when a 25 °C liquid jet impinges on the hot surface where surface having surface heat flux of 134 MW/m^2. It is found that the value of T_{lavg} lies well below the homogeneous bubble nucleation temperature if the contact time is less than 10 μs. Therefore, for the initiation of homogeneous bubble nucleation requires the impinging liquid to be in contact for more than 10 μs for prescribed heat flux boundary condition. For the other cases, as shown in Fig. 2, the requisite contact times for homogeneous bubble nucleation varies as explained above during describing Fig. 2.

4. CONCLUSIONS

A theoretical model to explicate the heat conduction phenomena during jet impingement quenching has been developed to get some information on the possibility of homogeneous bubble nucleation. The model has been solved numerically where three different cases have been considered. The following speculations can be devised from this study:

(a) A contact of 10 μs is required to initiate homogeneous bubble nucleation for the cases where the impinging surface releases constant heat to the impinging liquid and its surface temperature drops at a certain rate depending on time.

(b) For the PST case, the values of T_{lavg}, r_e and $\bar{u}$ depend on material. But, for the PHF and TST cases, they are not material dependent.

(c) An accurate knowledge of the size of the vapor bubbles, number of molecules in a vapor bubble and the energy required to initiate bubble formation needs further investigation.

5. REFERENCES

1. Wolf, D.H., Incropera, F.P., Viskanta, R., Jet impingement boiling, Advances in Heat Transfer 23, pp.1-132 (1993).
2. Piggott, B.D.G., White, E.P. and Duffey, R.B., Wetting delay due to film and transition boiling on hot surfaces, Nucl. Eng. Des. 36, pp. 169–181 (1976).
3. Hammad, J., Monde, M. and Mitsutake, Y., Characteristics of heat transfer and wetting front during quenching by jet impingement, Therm. Sci. Eng. 12, pp. 19–26 (2004).
4. Woodfield, P.L., Monde, M. and Mozumder, A.K., Observations of high temperature impinging-jet phenomena, Int. J. Heat Mass Transfer 48, pp. 2032-2041 (2005).
5. Mozumder, A.K., Monde, M., and Woodfield, P.L., Delay of wetting propagation during jet impingement quenching for a high temperature surface, Int. J. Heat Mass Transfer 48, pp. 5395-5407(2005).
6. Islam, M.A., Woodfield, P.L., Mozumder, A.K., Mitsutake, Y., and Monde, M., Boiling and wetting phenomena of hot surface during jet impingement quenching, Proc. 13-IHTC, Sydney, Australia, (2006).
7. MA Islam, M Monde, PL Woodfield and AK Mozumder, "Jet impingement quenching phenomena for hot surfaces well above the limiting temperature for solid-liquid contact," *Int. J. Heat and Mass Transfer* (2006) (in press).
8. Islam, M.A., Monde, M, Woodfield, P.L., Mitsutake, Y and Mozumder, A.K., Jet impingement boiling in hot surfaces well above the limiting temperature for solid-liquid contact, Multiphase Science and Technology, Vol. 19, No. 2, pp. 167-181, 2007.
9. H. S. Carslaw and J. C. Jaeger, Conduction of heat in solids, Second edition, Oxford University Press, 2001, pp. 87-89.
10. V. P. Carey, Liquid-vapor phase change phenomena, Taylor and Francis, Copyright © 1992 by Hemisphere Publishing corporations.
11. Y. Iida, K. Okuyama and K. Sakuri, "Boiling nucleation on a very small film heater subjected to extremely rapid heating," *Int. J. Heat and Mass Transfer* (1994).

6. NOMENCLATURE

Symbol	Meaning	Unit
A	Thermal diffusivity of liquid	(m^2/s)
c	Specific heat of liquid	(J/mole/K)
q	Heat flux	(MW/m^2)
x_e	the liquid depth equal to the diameter of the critical vapor embryo in the superheated liquid	(m)
r_e	Radius of the critical vapor embryo	(m)
T_l	Liquid Initial Temperature	(^{o}C)
T_{lavg}, $\bar{T}$	Average Liquid Temperature	(^{o}C)
u	Energy stored in the liquid	(J/molecul)
$\bar{u}$	Average energy stored in the liquid	(J/molecul)
λ	Thermal Conductivity of Solid	(W/m/K)
t	Time elapsed	(s)
k	Rate of change in surface temperature	(K/s)
P_{sat}	Saturation pressure	(Pa)
P_∞	Ambient pressure	(Pa)
σ	Surface tension	(N/m)
R	Universal Gas Constant	(J/K/mol)